Atomic Resolution Imaging and Topography of Boron Nitride Sheets Produced by Chemical Exfoliation

Jamie H. Warner,[†,*] Mark H. Rümmeli,[‡] Alicja Bachmatiuk,[‡] and Bernd Büchner[‡]

[†]Department of Materials, University of Oxford, Parks Rd, Oxford OX1 3PH, United Kingdom, and [‡]IFW Dresden, P.O. Box 270116, D-01171 Dresden, Germany

ABSTRACT Here, we present a simple method for preparing thin few-layer sheets of hexagonal BN with micrometer-sized dimensions using chemical exfoliation in the solvent 1,2-dichloroethane. The atomic structure of both few-layer and monolayer BN sheets is directly imaged using aberration-corrected high-resolution transmission electron microscopy. Electron beam induced sputtering effects are examined in real time. The removal of layers of BN by electron beam irradiation leads to the exposure of a step edge between a monolayer and bilayer region. We use HRTEM imaging combined with image simulations to show that BN bilayers can have AB stacking and are not limited to just AA stacking.

KEYWORDS: boron nitride · HRTEM · nanomaterials · BN · aberration-corrected · 2D crystal

The exfoliation of 3D layered materials into their 2D sheet-like counterpart can lead to new material properties that are unique to the 2D crystal.[1] The exfoliation of graphite to graphene monolayers is the best example so far of the wealth of new properties that can emerge.[2,3] Other layered structures, such as boron nitride (BN), can also be exfoliated to form unique 2D crystal structures.[1] However, unlike graphene, the potential novel physical properties that could emerge in monolayer BN are yet to be elucidated. This is primarily due to the limited number of reported synthetic approaches for preparing thin few-layer and monolayer sheets.[4−6] Isolating individual monolayer sheets of 2D crystals also enables characterization of the topography and new insights into the dynamic behavior of lattice defects and edge states to be unravelled.

Boron nitride exhibits high thermal stability, deep ultraviolet photon emission, good mechanical strength, and has been utilized as a solid-state lubricant.[7−9] BN nanotubes have been produced, and subsequent studies have shown they are noncytotoxic.[10,11] BN sheets with nanostructure in the form of a highly ordered nanomesh have been synthesized using self-assembly on a Ru(111) single-crystal surface.[12] BN consists of pairs of boron and nitrogen atoms that are isoelectronic to pairs of carbon atoms. BN can adopt several phases such as hexagonal, sphalerite, wurtzite, cubic, and rhombohedral. In hexagonal BN, the lattice structure of a single monolayer is similar to graphene, except with alternating boron and nitrogen atoms in the hexagons. The layering of the basal plane of the sheets to form a 3D solid can adopt several arrangements, but in contrast to the AB stacking in graphite, AA′ stacking is the suggested preference.[13−15] However, the difference in cohesive energy between several different stacking symmetries is small, and this indicates that basal plane sliding may occur, leading to the possibility of non-AA′ stacking in BN sheets.[16]

RESULTS AND DISCUSSION

Here, we use a novel chemical exfoliation method consisting of sonicating boron nitride powder in 1,2-dichloroethane for 3 h to produce few-layer hexagonal BN sheets with micrometer-sized dimensions. This approach builds upon our recent work on exfoliating graphite to produce few-layer graphene sheets.[17,18] 1,2-Dichloroethane has the advantage over other solvents previously used for chemical exfoliation of BN such as dimethylformamide (DMF) by having a lower boiling point, ensuring that removal of solvent is rapid and simple.[5] Figure 1a shows a typical micrometer-sized sheet of exfoliated BN sitting on the lacey carbon grid. Figure 1b shows a region of the surface of the BN sheet with higher resolution with the hexagonal atomic structure of BN observed. Figure 1c shows a HRTEM image with a large area of the atomic structure clearly visible. This section of the BN sheet contained

*Address correspondence to jamie.warner@materials.ox.ac.uk.

Received for review May 27, 2009 and accepted February 01, 2010.

Published online February 11, 2010. 10.1021/nn901648q

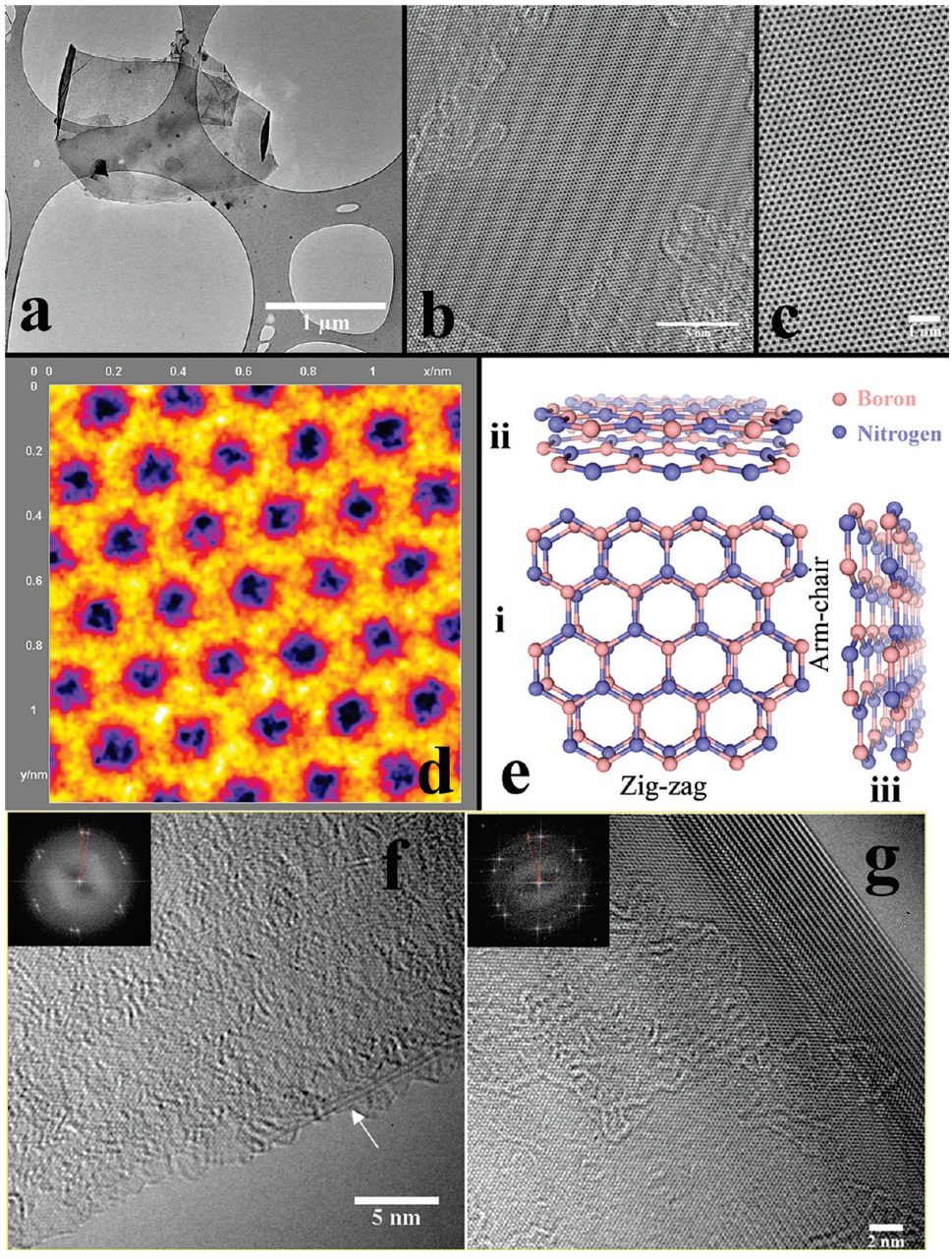

Figure 1. (a) TEM image of an exfoliated BN sheet. (b) HRTEM image of the surface of a multilayered BN sheet. (c) HRTEM image of a multilayered BN sheet with atomic structure. (d) HRTEM image in color with the B−N bond resolved. (e) Structural diagram of AA′ stacked BN sheet (i) top view, (ii) end view, and (iii) side view. (f) Edge of a BN sheet with 2−3 layers. Inset shows 2D fast Fourier transform (FFT). Red lines indicate angle of rotation. (g) Folded edge of a BN sheet with 10 layers. Inset shows 2D FFT. Red lines indicate angle of rotation.

several layers (*i.e.*, 5−10). Our resolution was sufficient to resolve the ~1.45 Å B−N bond and image the full atomic structure. Figure 1d shows a HRTEM image presented in false color for enhanced visual effect. It is generally accepted that hexagonal boron nitride adopts AA′ stacking, in contrast to the AB stacking well-known for graphite. Figure 1e presents an atomic structural diagram of BN sheets with AA′ stacking, with (i) top view, (ii) end view, and (iii) side view. The top view in Figure 1e(i) presents the BN sheets with zigzag atomic termination for the top and bottom edges and armchair atomic termination for the left and right sides. The phase contrast observed in the HRTEM images in Figure 1c,d would be produced for BN sheets with AA′ stacking and also for AB stacking.

Insights into the number of layers in the BN sheets can be achieved by examining the edges. Figure 1f shows the edge of a BN sheet with between 2 and 3 layers. An arrow in Figure 1f indicates two straight lines of contrast that could be due to back-folding of a bilayer of BN. The inset in Figure 1f presents the 2D fast Fourier transform (FFT) taken from the HRTEM image. Twelve spots are observed with 0.21 nm *d* spacing, which corresponds to two sets of six spots with a rotation of 7.7° between them. This indicates that there is deviation from the AA′ BN stacking arrangement. This is similar to the recently imaged rotational stacking faults in few-layer graphene sheets.[18] Rotational stacking faults are typically associated with back-folding of a sheet. Figure 1g shows a back-folded edge of a BN sheet with 10 layers. Straight lines at the edge are observed, typical of folded edges. The inset in Figure 1g presents the 2D FFT and reveals that the back-folding has induced a rotation of 16.8° between the bottom 10 layers and the top 10 layers. The folded edge enables the interlayer spacing, d_s, to be measured directly using 2D FFT analysis as $d_s = 0.325 \pm 0.01$ nm, which is close to that in bulk hexagonal BN crystals.

The knock-on damage threshold of boron and nitrogen atoms in BN sheets is slightly lower than that of carbon atoms in graphene sheets. Zobelli *et al.* calculated a threshold of 74 keV for boron atoms and 84 keV for nitrogen atoms in BN nanotubes.[19] They predict an accelerating voltage of 80 kV should first generate boron vacancies followed by the removal of neighboring nitrogen atoms surrounding the defect. We observed that electron beam irradiation resulted in the formation of defects in the few-layer BN sheets that evolved into

triangular nanopatterns. The nanopatterning is due to boron and nitrogen atoms being ejected *via* electron beam induced sputtering from the BN sheet, most likely from the back surface monolayer. Ejection of atoms *via* electron beam induced sputtering generally occurs from the back surface in the same direction as the incident electron due to the larger transfer of momentum in this direction to the stationary atom.[20] Figure 2(i)a shows a region of the BN sheet after 2 min of electron beam irradiation with a beam current density of ~0.1 pA/nm^2. A large number of triangular nanopatterns are observed, and these correspond to regions of the BN sheet with loss of material and subsequent reduced contrast in the HRTEM images. A 2D FFT is included in the bottom right inset of Figure 2(i)a with six spots apparent. The spots indicate the direction of the arm-chair orientation of the BN lattice, and the arrows show the direction of the zigzag orientation. The triangular nanopatterns in Figure 2(i)a are primarily terminated with zigzag edges. Figure 2(i)b shows the same area after a further 30 s of electron beam irradiation. The region of BN sheet sputtered away has grown, and the sizes of the triangles have increased. This shows that boron and nitrogen atoms are removed along the zigzag row, enabling the triangles to grow and retain their shape during the evolution.

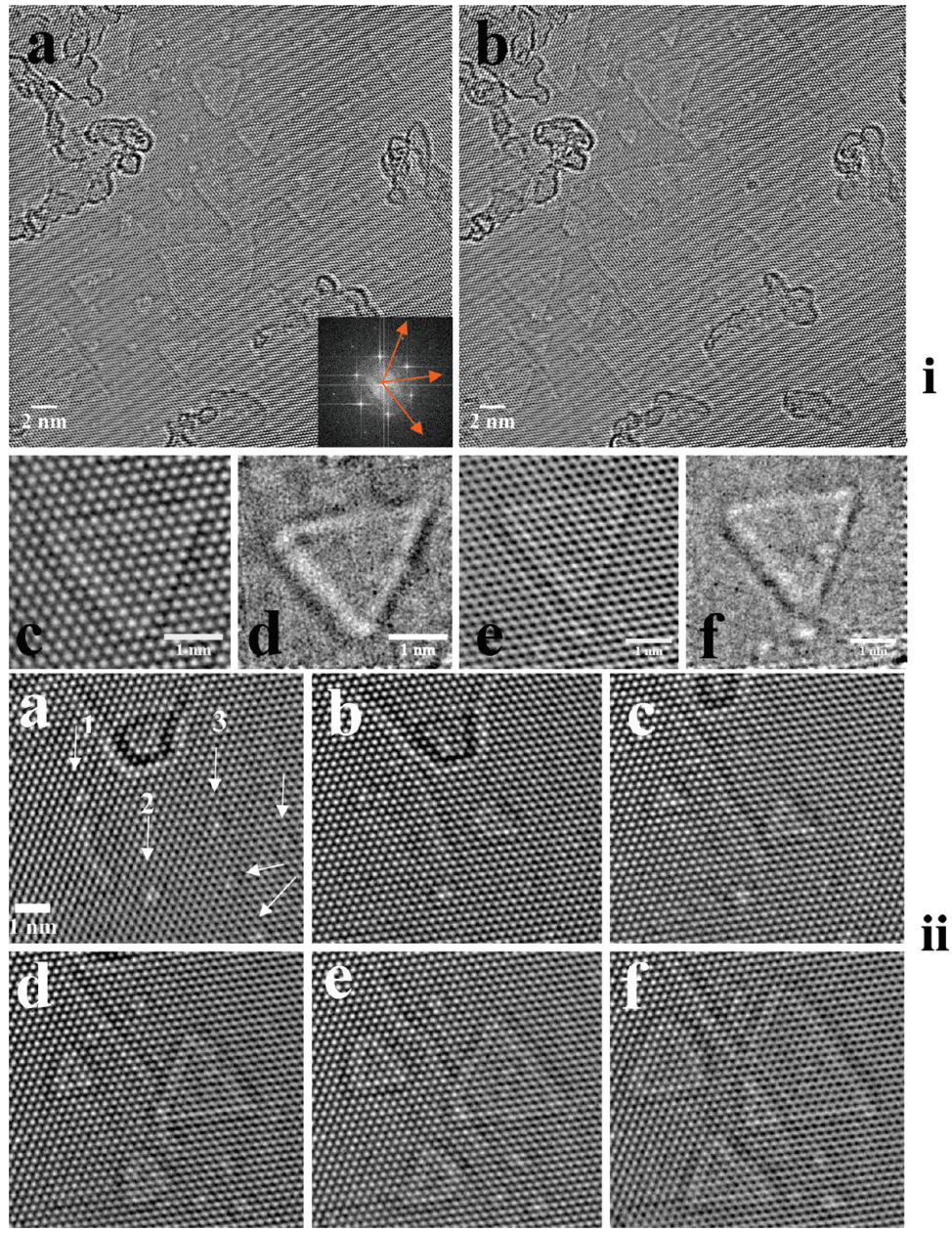

Figure 2. (i) (a) TEM image showing triangular nanopatterns formed by electron beam induced sputtering; inset shows 2D FFT with arrows indicating zizzag orientation. (b) Same area as in (a), after 20 s of further irradiation. (c) HRTEM image of a triangular nanopattern. (d) HRTEM image presented in (c) after removing BN lattice structure by Fourier filtering. (e) HRTEM image of another triangular nanopattern. (f) HRTEM image presented in (e) after removing BN lattice structure by Fourier filtering. (ii) Time series of HRTEM images showing the growth of triangular nanopatterns from initial defects in the BN lattice caused by electron beam irradiation, time between images = 20 s.

Figure 2(i)c shows a triangle with sides of nearly 2 nm each. In Figure 2(i)d, the lattice structure of the BN sheet is removed by Fourier filtering. A similar process is done for the equilateral triangle shown in Figure 2(i)e,f. The triangular nanopatterns grow from initial defects produced in the BN sheet by electron beam irradiation, and according to the theory of Zobelli *et al.*, these are most likely boron vacancies.[19] Figure 2(ii) shows a HRTEM of a region of BN sheet containing several initial defects produced by the electron beam, indicated with arrows. Figure 2(ii)a−f shows a time series of HRTEM images with 20 s between frames. In Figure 2(ii)b, defect 3 has evolved and transformed into a small triangle. As time progresses, defects 1, 2, and 3 all grow into triangular nanopatterns with edges along the zigzag orientation. This shows the initial stage of the triangle nanopatterning forming from defects produced by electron beam irradiation.

Previous work has shown that BN has a tendency to form triangular nanostructures that are terminated with nitrogen atomic zigzag edges.[21,22] Jin and co-

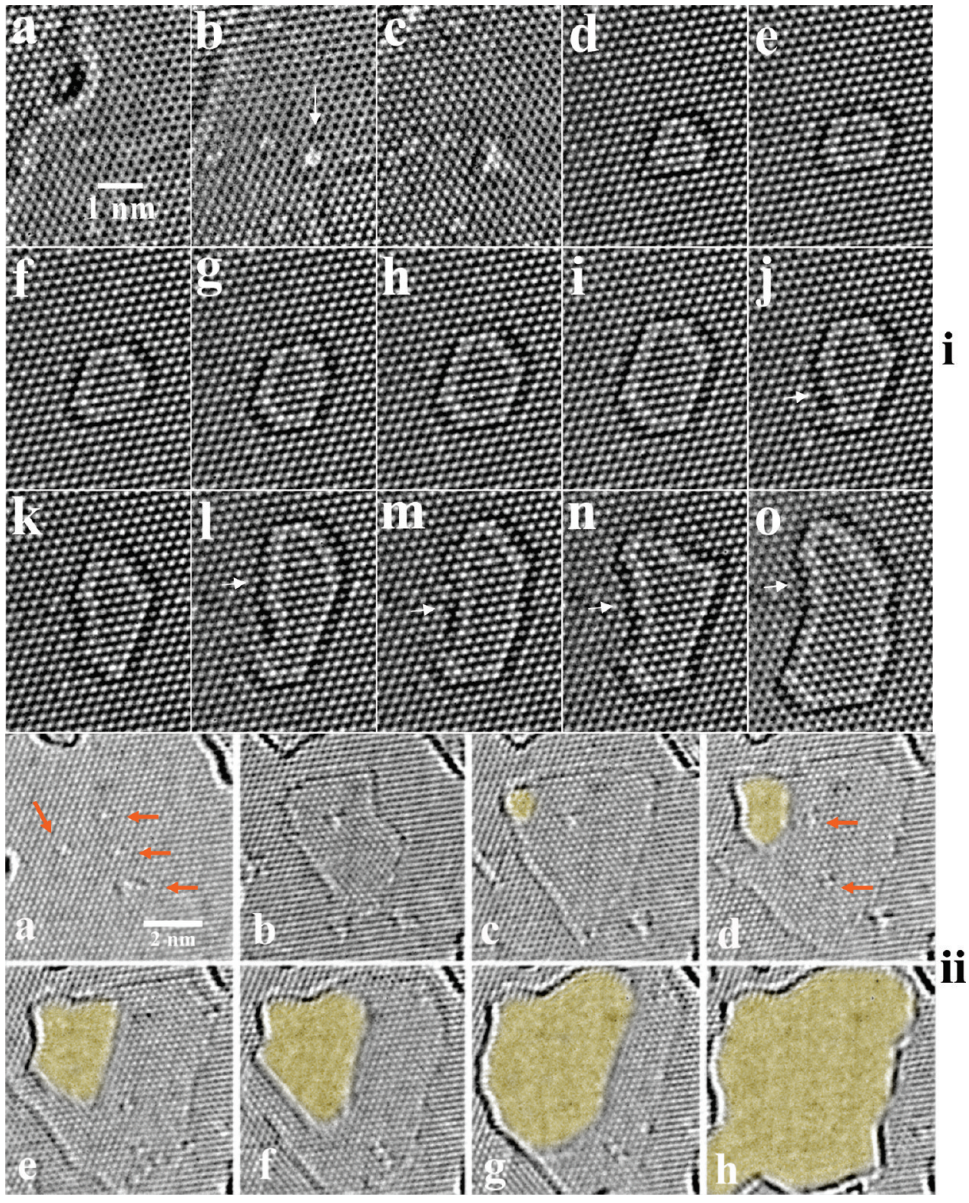

Figure 3. (i) Time series of HRTEM images (a−o) showing the formation of a hexagonal vacancy in one layer of BN in the multilayered structure. Time between frames is 5 s. (ii) Time series of HRTEM images of a BN bilayer under electron beam irradiation. Time between frames is 20 s. Gold shading highlights the formation of a freespace hole in the monolayer.

workers prepared freestanding BN single layers by electron beam thinning and analyzed the defects using HRTEM exit wave reconstruction to identify individual B and N atoms.[23] They observed that defects formed by electron beam irradiation adopted triangular shapes, similar to what we have observed in Figure 2, even though an accelerating voltage of 120 kV was used, above the knock-on damage threshold for both B and N atoms.[23] We have used an accelerating voltage of 80 kV, which should be sufficient to remove B atoms, but not N atoms, due to difference in the knock-on damage threshold. Since our initial submission, Meyer *et al.* and Alem *et al.* have also observed the formation of triangular defects in BN sheets using 80 kV electron beam irradiation.[23,24] All reports of electron beam induced defects in BN sheets show that they are produced on the same sublattice within a monolayer and are due to the preferential sputtering of boron atoms.[21−23] This results in zigzag edges that are terminated by nitrogen atoms.[23−25]

The triangular nanopatterning in Figure 2 is attributed to atoms surrounding defects having dangling bonds, which are easier to sputter out the back surface by electron beam induced knock-on energy transfer.[17,26] This is similar to recent observations of zigzag edges of holes in graphene layers.[26] However, the effects observed in BN sheets are far more pronounced. The ability to remove large areas within BN sheets opens up the possibility to explore step edges between monolayer and bilayer regions in BN sheets.

In some cases, the defect evolved into a hexagonal rather than triangular pattern. Figure 3(i) presents a time series of HRTEM images of such a case. Figure 3(i)a shows the multilayered BN sheet at the beginning of the irradiation and 5 s later, and in Figure 3(i)b, a new defect has been formed, indicated with an arrow. Between Figure 3(i)d and 3(i)i, the defect adopts hexagonal structure and grows with purely zigzag edges. However, in Figure 3(i)j, the total area of the structure decreases as the bottom left edge adjusts from zigzag to arm-chair termination, indicated with an arrow. This change in shape proves that structural reconfiguration of the edges occurs during the sputtering process. As the structure gets larger, between Figure 3(i)j and 3(i)o, arm-chair edges are still apparent, shown with arrows. The larger structures develop more edges and no longer have six sides.

Figure 3(ii)a shows a bilayer region of BN with four defects apparent, indicated by arrows. Figure 3a−h presents a time series of HRTEM images showing the effect of electron beam irradiation. Figure 3b shows that a region of one of the monolayers has been sputtered away, leaving behind a single monolayer containing a

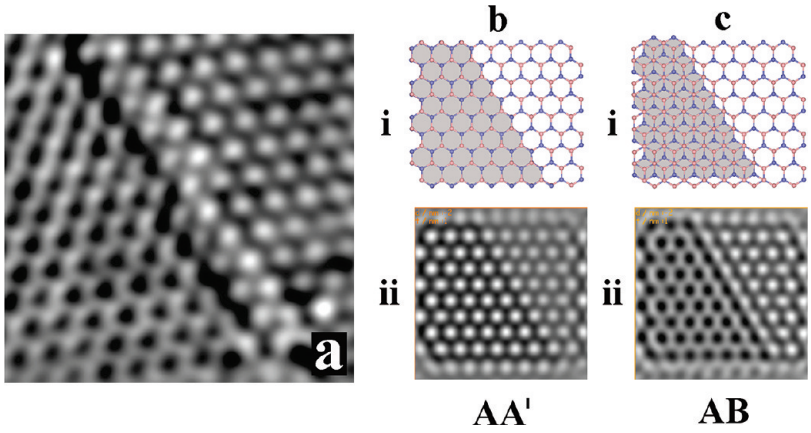

Figure 4. (a) HRTEM image of the step edge between monolayer and bilayer region, showing AB stacking. (b) Step edge of AA′ stacked BN bilayer. (i) Atomic structural representation, gray area indicates the size of the top BN sheet. (ii) HRTEM image simulation of the atomic structure presented in (i). (c) Step edge of AB stacked BN bilayer. (i) Atomic structural representation, gray area indicates the size of the top BN sheet. (ii) HRTEM image simulation of the atomic structure presented in (i).

defect. In Figure 3c, the area has formed a triangular shape and a hole has appeared in the monolayer, highlighted in gold. In Figure 3d, the hole has grown in size and two new defects are apparent in the monolayer region, indicated with arrows. This is clear evidence that defects are produced in areas of BN that were previously defect-free by electron beam irradiation. The size of the monolayer region has also increased. Figure 3e−h shows that the hole in the monolayer increases steadily in size until it reaches the edge of the bilayer. The edge of the hole in the monolayer shows termination along the zigzag orientation.

Finally, we examine the step edge between a monolayer and bilayer in BN to provide insights into the packing structure of few-layer BN sheets. Figure 4a shows a HRTEM image of the step edge between a monolayer region on the top right and a bilayer region on the bottom left. The step edge runs through the middle at ~45°. The bilayer region shows white hexagonal atomic structure, while the monolayer region shows black hexagonal atomic structure. Furthermore, there is an offset between the white zigzag rows and the black zigzag rows between the monolayer and bilayer. In order to interpret this, we performed multislice HRTEM image simulations. Figure 4b(i) shows the atomic structure used in a supercell simulation for AA′ stacking with the top bilayer region indicated by gray shading and a step edge running through the middle at 45°. The HRTEM image simulation of this structure is shown in Figure 4(ii)b. Figure 4(i)c shows the atomic structure for AB stacking, with the image simulation shown in Figure 4(ii)c. Comparing the HRTEM image simulations for AA′ and AB stacking reveals two major differences. AA′ stacked BN (Figure 4(ii)b) has the same contrast for both the monolayer and bilayer region (black). AB stacked BN has opposite contrast for the monolayer (black) and bilayer (white). The atomic structure along the zigzag orientation for AA′ stacking is continuous, whereas for AB stacking, there is an offset. The HRTEM image presented in Figure 4a can be matched to the image simulation for AB stacked BN and not to AA′ stacking. Thus, our HRTEM analysis has shown that AB stacking is possible for bilayer regions of BN sheets. This AB stacking may not be intrinsic to the bulk samples and may be only possible at the top and bottom of the layered structure where single BN sheets can slide easily. Sonication of the BN sheets may also play a role in enabling the end sheets to adjust from AA′ to AB stacking. We did not find any detectable evidence for ripples within the BN sheets that could have led to the AB stacking.

CONCLUSION

Our simple chemical exfoliation method enabled the detailed study of multilayered and monolayer hexagonal BN. Even at the low accelerating voltage of 80 kV, knock-on structural damage was still apparent and resulted in newly formed defects in regions of BN that were originally pristine. Under continuous irradiation, these defects evolve into triangular nanopatterns with predominantly zigzag edge termination and occasionally hexagonal structures. We observed dynamic structural changes in the edges of the holes with reconfiguration from a zigzag to an arm-chair edge. The ability to resolve the B−N bond sheds important light on the atomic structure of BN sheets that will be important in the future development of 2D crystals of hexagonal BN and the understanding of the novel properties that may emerge.

EXPERIMENTAL METHODS

Thin sheets of hexagonal boron nitride were prepared by dispersing 0.1 mg of *h*-BN powder (Sigma Aldrich) in 5 mL of 1,2-dichloroethane using an ultrasonic bath for 3 h. The solution was left to rest for 30 min to allow large particles to settle to the bottom of the vial. A laceycarbon coated TEM grid was dipped into the top of the solution and left to dry. Low-voltage aberration-corrected high-resolution transmission electron microscopy was performed using a FEI Titan^3, operating at an accelerating voltage of 80 kV, with spherical aberration correction. Multislice image simulations were performed using JEMS software, with C_s = −0.04 mm, defocus spread = 11.0 nm, and defocus of 8 nm.

Supercells for the step edges of AA′ and AB stacked bilayers were constructed using Accelrys DS Viewer Pro. HRTEM image processing was performed using Image J software.

Acknowledgment. J.H.W. thanks the Violette and Samuel Glasstone Fund and Brasenose College, University of Oxford, for the support.

REFERENCES AND NOTES

1. Novoselov, K. S.; Jiang, D.; Schedin, F.; Booth, T. J.; Khotkevich, V. V.; Morozov, S. V.; Geim, A. K. Two-Dimensional Atomic Crystals. *Proc. Natl. Acad. Sci. U.S.A.* **2005**, *102*, 10451–10453.
2. Geim, A. K.; Novoselov, K. S. The Rise of Graphene. *Nat. Mater.* **2007**, *6*, 183–191.
3. Novoselov, K. S.; Geim, A. K.; Morozov, S. V.; Jiang, D.; Zhang, Y.; Dubonos, S. V.; Grigorieva, I. V.; Firsov, A. A. Electric Field Effect in Atomically Thin Carbon Films. *Science* **2004**, *306*, 666–669.
4. Pacile, D.; Meyer, J. C.; Girit, C. O.; Zettl, A. The Two-Dimensional Phase of Boron Nitride: Few-Atomic-Layer Sheets and Suspended Membranes. *Appl. Phys. Lett.* **2008**, *92*, 133107.
5. Zhi, C.; Bando, Y.; Tang, C.; Kuwahara, H.; Golberg, D. Large-Scale Fabrication of Boron Nitride Nanosheets and Their Utilization in Polymeric Composites with Improved Thermal and Mechanical Properties. *Adv. Mater.* **2009**, *21*, 1–5.
6. Han, W.-Q.; Wu, L.; Zhu, Y.; Watanabe, K.; Taniguchi, T. Structure of Chemically Derived Mono- and Few-Atomic-Layer Boron Nitride Sheets. *Appl. Phys. Lett.* **2008**, *93*, 223103.
7. Han, W.-Q.; Mickelson, W.; Cumings, J.; Zettl, A. Transformation of $B_xC_yN_z$ Nanotubes to Pure BN Nanotubes. *Appl. Phys. Lett.* **2002**, *81*, 1110.
8. Kubota, Y.; Watanabe, K.; Tsuda, O.; Taniguchi, T. Deep Ultraviolet Light-Emitting Hexagonal Boron Nitride Synthesized at Atmospheric Pressure. *Science* **2007**, *317*, 932–934.
9. Golberg, D.; Costa, P. M. F. J.; Lourie, O.; Mitome, M.; Bai, X.; Kurashima, K.; Zhi, C.; Tang, C.; Bando, Y. Direct Force Measurements and Kinking under Elastic Deformation of Individual Multiwalled Boron Nitride Nanotubes. *Nano Lett.* **2007**, *7*, 2146–2151.
10. Chopra, N. G.; Luyken, R. J.; Cherrey, K.; Crespi, V. H.; Cohen, M. L.; Louie, S. G.; Zettl, A. Boron Nitride Nanotubes. *Science* **1995**, *269*, 966–967.
11. Chen, X.; Wu, P.; Rousseas, M.; Okawa, D.; Gartner, Z.; Zettl, A.; Bertozzi, C. R. Boron Nitride Nanotubes Are Noncytotoxix and Can Be Functionalized for Interaction with Proteins and Cells. *J. Am. Chem. Soc.* **2009**, *131*, 890–891.
12. Corso, M.; Auwarter, W.; Muntwiler, M.; Tamai, A.; Greber, T.; Osterwalder, J. Boron Nitride Nanomesh. *Science* **2004**, *303*, 217–220.
13. Pease, R. S. Crystal Structure of Boron Nitride. *Nature* **1950**, *165*, 722–723.
14. Kern, G.; Kresse, G.; Hafner, J. *Ab Initio* Calculation of the Lattice Dynamics and Phase Diagram of Boron Nitride. *Phys. Rev. B* **1999**, *59*, 8551–8559.
15. Yu, W. J.; Lau, W. M. *Ab Initio* Study of Phase Transformations in Boron Nitride. *Phys. Rev. B.* **2003**, *67*, 014108.
16. Ooi, N.; Rairkar, A.; Lindsley, L.; Adams, J. B. *J. Phys.: Condens. Matter* **2006**, *18*, 97–115.
17. Warner, J. H.; Rummeli, M. H.; Ge, L.; Gemming, T.; Montanari, B.; Harrison, N. M.; Buchner, B.; Briggs, G. A. D. Structural Transformations in Graphene Studied with High Spatial and Temporal Resolution. *Nat. Nano* **2009**, *4*, 500–504.
18. Warner, J. H.; Ruemmeli, M. H.; Gemming, T.; Buechner, B.; Briggs, G. A. D. Direct Imaging of Rotational Stacking Faults in Few Layer Graphene. *Nano Lett.* **2009**, *9*, 102–106.
19. Zobelli, A.; Gloter, A.; Ewels, C. P.; Seifert, G.; Colliex, C. Electron Knock-On Cross Section of Carbon and Boron Nitride Nanotubes. *Phys. Rev. B* **2007**, *75*, 245402.
20. Egerton, R. F.; Li, P.; Malac, M. Radiation Damage in the TEM and SEM. *Micron* **2004**, *35*, 399–409.
21. Xu, L.; Zhan, J.; Hu, J.; Bando, Y.; Yuan, X.; Sekiguchi, T.; Mitome, M.; Golberg, D. High Yield Synthesis of Rhombohedral Boron Nitride Triangular Nanoplates. *Adv. Mater.* **2007**, *19*, 2141–2144.
22. Auwtrer, W.; Suter, H. U.; Sachdev, H.; Greber, T. Synthesis of One Monolayer of Hexagonal Boron Nitride on Ni (111) from B-Trichloroborazine $(ClBNH)_3$. *Chem. Mater.* **2004**, *16*, 343–345.
23. Jin, C.; Lin, F.; Suenaga, K.; Iijima, S. Fabrication of a Freestanding Boron Nitride Single Layer and Its Defect Assignments. *Phys. Rev. Lett.* **2009**, *102*, 195505.
24. Meyer, J. C.; Chuvilin, A.; Algara-Siller, G.; Biskupek, J.; Kaiser, U. Selective Sputtering and Atomic Resolution Imaging of Atomically Thin Boron Nitride Membranes. *Nano Lett.* **2009**, *9*, 2683–2689.
25. Alem, N.; Erni, R.; Kisielowski, C.; Rossell, M. D.; Gannett, W.; Zettl, A. Atomically Thin Hexagonal Boron Nitride Probed by Ultrahigh-Resolution Transmission Electron Microscopy. *Phys. Rev. B* **2009**, *80*, 155425.
26. Girit, C. O.; Meyer, J. C.; Erni, R.; Rossell, M. D.; Kisielowski, C.; Yang, L.; Park, C.-H.; Crommie, M. F.; Cohen, M. L.; Louie, S. G.; Zettl, A. Graphene at the Edge: Stability and Dynamics. *Science* **2009**, *323*, 1705–1708.